UNIVERSITAT DE BARCELONA

MASTER FINAL PROJECT
MASTER OF ENVIRONMENTAL ENGINEERING

Role of oxygen in sunlight induced photodegradation of organophosphorous flame retardants in river waters

Author

Alberto Cruz Alcalde

June 2016

Director

Dr. Carme Sans Mazón
Departament d'Enginyeria Química i Química Analítica
Universitat de Barcelona

Abstract

The persistence of organophosphorous flame retardants (OPFR) on the aquatic environment has motivated the study of their degradation processes in superficial water, particularly the sunlight induced photodegradation mechanisms. A recent study showed that some of these substances, with a low capacity for solar radiation absorption, became surprisingly photodegraded. Indirect photolysis promoted by the photosensitizer properties of this micropollutants constitutes a suitable explanation for this phenomenon.

The objective of this project was to investigate the photodegradation indirect mechanisms of OPFR in superficial water, in which singlet oxygen ($^1O_2$) appeared to develop an important role. By means of two different procedures, chemical probe photobleaching and spin-trapping experiments, the specific aim was the detection and identification of this species in the reaction medium.

Although photobleaching procedures applied to monitor reactions involving singlet oxygen have been widely used, the reported experimental conditions are quite different from the ones required to observe OPFR photosensitizing effects. Thus, several assays were carried out in first place in order to adapt the experimental settings. In spite of that, results did not shown clear evidences about the generation of singlet oxygen during the experiments, regardless of the chemical probe employed. The great competence for singlet oxygen, stablished in the reaction medium, seems to minimize the concentration of this species in there, thus making difficult its detection.

For their part, spin-trapping procedures demonstrated to be useful to reliably detect and identify the singlet oxygen molecules generated along the process. Because of its high sensitivity to excited structures, this method allows to effectively detect the presence of $^1O_2$, even when this species is present at very low concentrations in the bulk solution.

Index

List of Figures

Nomenclature

Abbreviations

4-o-TEMP	2,2,6,6-Tetramethyl-4-piperidone
4-oxo-TEMPO	2,2,6,6-Tetramethyl-4-piperidone-1-oxyl
ABMDMA	9,10-Anthracenediyl-bis(methylene)dimalonic acid
ADPA	9,10-Anthracenedipropionic
EHDP	2-Ethylhexyl diphenyl phosphate
EPR	Electron paramagnetic resonance
ESR	Electron spin resonance
FFA	Furfuryl alcohol
HPLC	High performance liquid chromatography
OPFR	Organophosphorous flame retardants
ROS	Reactive oxygen species
SS	Steady state
TMPP	Trimethyl phenyl phosphate
UV	Ultraviolet
UV-Vis	Ultraviolet-visible
WWTP	Wastewater treatment plant

Symbols

^{14}O	Oxygen isotope with mass number 14
^{16}O	Oxygen isotope with mass number 16
$^{1}O_2$	Singlet oxygen
B	Magnetic field [G]
E	Energy [J]
G	Gauss, unit of magnetic field [10^{-4} kg·s^{-2}·A^{-1}]
g	Proportionality factor or *g-factor*
h	Planck constant [J·s]

I	Magnetic nuclei spin number
ka	Specific light absorbance of the reaction medium [mol photons absorbed$^{-1}\cdot s^{-1}$]
kd	Rate of decay of singlet oxygen back to its ground state due to quenching by water [mol $^1O_2\cdot L^{-1}\cdot s^{-1}$]
kx	Reaction rate between singlet oxygen and X [s^{-1}]
M_S	Unpaired electron spin number
N	Number of equivalent magnetic nuclei
O_2	Molecular oxygen
$O_2^{-}\cdot$	Superoxide radical
$OH\cdot$	Hydroxyl radical
S	Photosensitizer species
T	Tesla, unit of magnetic field [$kg\cdot s^{-2}\cdot A^{-1}$]
X	Generic chemical species present at the reaction medium
Xe	Xenon
ΔE	Energy difference [J]
μ	Magnetic moment of the electron [$J\cdot T^{-1}$]
μ_B	Bohr magneton [$J\cdot T^{-1}$]
ν	Radiation frequency [Hz]
Φ_{SO}	Singlet oxygen quantum yield of a photosensitizing species [mol $^1O_2$ generated $\cdot$ mol photons absorbed^{-1}]

1 Introduction

1.1 Emerging contaminants: organophosphorous flame retardants

Increasing public health concern has grown in relation to a relatively new group of pollutants, present at low concentrations in water systems. They are commonly known as emerging contaminants, since they are still in the process of being regulated and little is known about their potential negative effects on the environment. These substances are continuously released from industrial and wastewater treatment plants (WWTP) effluents to the aquatic media, and they are biologically recalcitrant. That is, current treatment technologies are very often unable to entirely degrade them [1], [2].

The emerging contaminants group is constituted by numerous chemical substances, including flame retardants employed in many household and industrial materials and final products [3], [4]. Particularly, the wide use of organophosphorous flame retardants (OPFR), which have become high production volume chemicals since polibrominated diphenil eters bans (see Figure 1) [4], has caused the release of important quantities of them into natural waters every day [3], [4], [5].

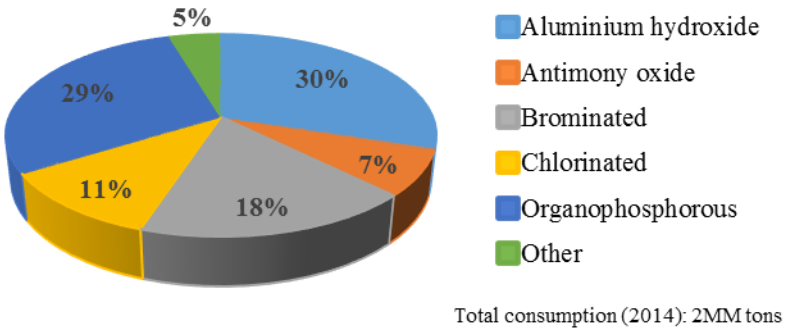

Figure 1. Global consumption of flame retardants in Plastics by type (2014) [6].

Since the mentioned situation does not appear to be convenient for human health and environment, the interest on studying the natural degradation processes of these compounds in superficial waters has increased during the last years, being sunlight induced phototransformations the most considered processes due to their demonstrated capability to deplete other biorrecalcitrant chemicals [2], [7].

1.2 Previous works on OPFR sunlight photodegradation

Some studies have been carried out on alkyl and chloroalkyl OPFR photodegradation under natural [8] and simulated [9] sunlight, showing low or even non-existent degradation levels.

A recent study [10] showed the degradation in water of an OPFR mixture (alkyl, chloroalkyl and aryl) exposed to natural sunlight. Since most of these compounds (alkyl and chloroalkyl) have low absorption within the solar spectrum radiation [10], and their high resistance to natural photodegradation has already been demonstrated, their phototransformation cannot be attributed to direct photolysis.

In this previous work it was indirectly demonstrated that photosensitizing promoted by the excitation of some light-absorption groups of OPFR molecules could be responsible for that phenomenon. Concretely, the degradation process may be attributed to singlet oxygen ($^1O_2$), a high reactive strong oxidant. It is thought that this species could be generated from the excitation of some OPFR containing aryl groups, since these ones present higher absorption levels than the others [10].

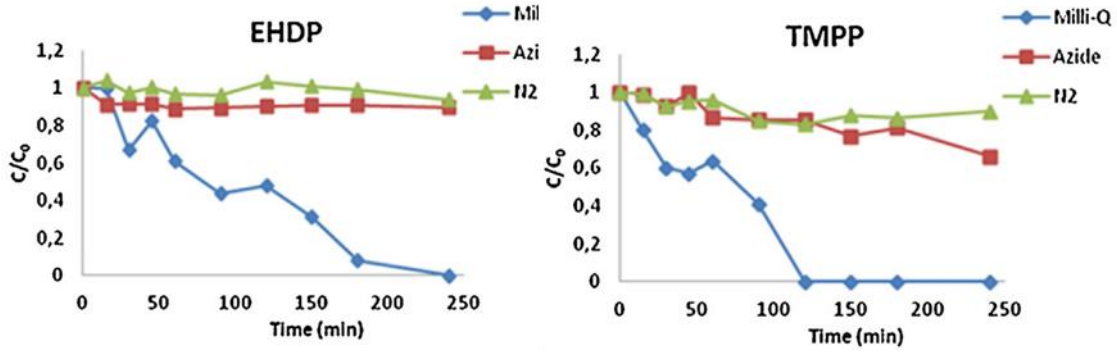

Figure 2. Photodegradation of EHDP and TMPP by simulated sunlight [10].

The examples (recovered from the previous work) shown in Figure 2 illustrates how two aryl OPFR diminished dramatically its photodegradation in absence of oxygen (by nitrogen bubbling) or in the presence of a well-known scavenger for singlet oxygen, sodium azide. As stated, this indirectly demonstrated that this species had to be involved on the natural photodegradation mechanism of OPFR.

1.3 Photolysis and photosensitization processes

When a chemical absorbs radiation, its excited molecules contain an excess of energy that can lead them to photochemical reactions, including photolysis. Basically, two general mechanisms of photolysis can be distinguished: direct photolysis, in which a chemical bond breaks into two parts, giving equal products or not; and indirect photolysis, carried out by natural and made-man compounds which have photosensitizing properties [11].

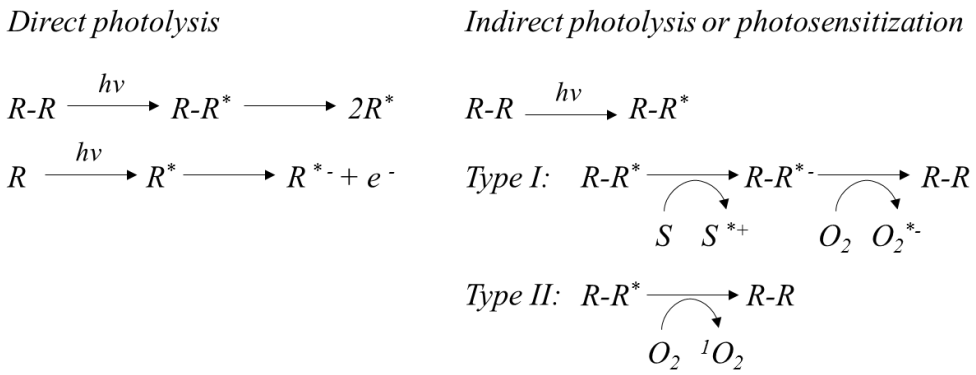

Figure 3. Main mechanisms for direct and indirect photolysis.

Photosensitizing occurs when a molecule is excited to the first or higher excited states after absorbing a light quantum. Sensitized excited triplet states are important radiation intermediates of organic molecules. Their relatively long lifetimes compared with their precursors excited singlet states allow to undergo bimolecular reactions. The excited triplet state may react in two ways, as shown in Figure 3. Type I mechanisms can involves electron or hydrogen atom transfer between the excited sensitizer and a substrate, yielding free radicals. These radicals can react with oxygen to form reactive oxygen species (ROS) like superoxide radical anion ($O_2^{-}\cdot$) or HO·, which have a wide range of reactivity with organic compounds. The excited triplet states can also directly react with other compounds present in the solution. Type II mechanisms involve energy transfer to molecular oxygen generating singlet oxygen ($^1O_2$). Each photosensitizer molecule can typically produce 10^3-10^5 molecules of $^1O_2$ before being degraded [10], [11].

Direct photolysis mechanism is practically limited to compounds that absorb radiation between 200-300 nm, that is, UV light with enough energy to directly break chemical

bonds. On the other hand, photosensitization processes can be initiated by lower energy radiation like UV-B, UV-A or even Visible light [12].

1.4 Justification and main hypothesis of the project

Surprising results from last reported study on OPFR natural photodegradation [10], as well as the scarcity of literature on this topic, have pointed the need of further research. Figure 4 shows the proposed reaction mechanism for the mentioned sunlight photodegradation process, according to the conclusions reached in the previous work and all the explanations above.

According to this process, OPFR would become excited by sunlight, in first place. Then, the excess of energy would be transferred to the dissolved oxygen from water, thus exciting its molecules and causing the generation of singlet oxygen. Finally, OPFR (same excited molecule turned back to its ground state or another one coming from the reaction medium) would react with singlet oxygen, yielding oxidation products.

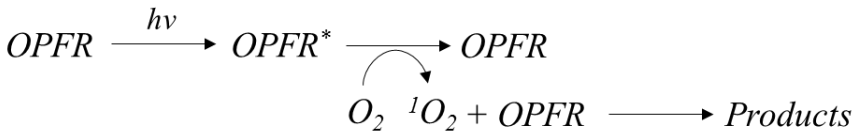

Figure 4. Hypothetical reaction pathway for natural photodegradation of OPFR.

Since this reaction pathway has not been directly demonstrated yet (there is only experimental evidence that needs to be confirmed), it constitutes the principal hypothesis of the current work and the main reason for its realization.

1.5 Photobleaching and Spin-trapping fundamentals

This part of the report is exclusively dedicated to provide some fundamentals about the two experimental procedures employed during the project: photobleaching experiments with chemical probe, on one hand, and spin-trapping experiments followed by EPR.

1.5.1 Photobleaching experiments

With the aim (as stated in the following section) of detecting singlet oxygen generation during OPFR phototransformation by sunlight, photobleaching experiments with chemical probe could be a proper experimental technique due to its (a priori) relative simplicity in terms of experimental setup and subsequent analysis.

Photobleaching implies irradiate chemical molecules of a photoactive compound in order to initiate a chemical process, with the intention of observing some effects or derived changes in the reaction medium. The role of the chemical probe on this assay is to prove that, effectively, this effect has taken place during the process. Thus, if photoinduced generation of singlet oxygen is wanted to be demonstrated from OPFR excitement, the experiment should follow the sequence illustrated in Figure 5.

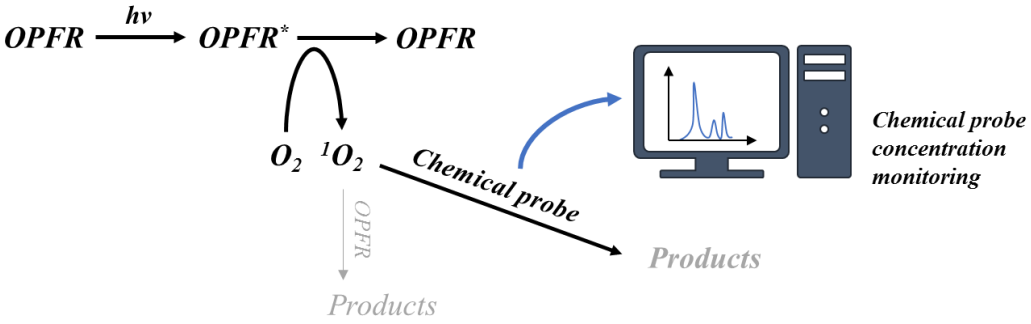

Figure 5. Scheme of a typical photobleaching experiment for $^1O_2$ detection.

The process of interest is represented in bold letters. The bulk solution is irradiated by simulated sunlight, and then the photosensitization process takes place. At this point, the chemical probe should react specifically (or present fast kinetics, at least) with singlet oxygen, thus diminishing its presence in the reaction medium. Since this decrease would be enough to demonstrate the generation of $^1O_2$ during the process, the concentration of the chemical probe is the parameter that must be monitored along the reaction.

1.5.2 Spin-trapping experiments

Since a spin-trapping experiment and subsequent analysis by EPR spectroscopy is a quite complicated and uncommon experimental procedure, an introduction to its fundamentals

is highly required for a good comprehension of this work. With this purpose, the basis of EPR spectroscopy are described in first place, followed by a brief resume of the spin-trapping procedure that should be carried out in the current case of study.

EPR Spectroscopy fundamentals

Electron paramagnetic resonance (EPR) spectroscopy, also referred to as electron spin resonance (ESR) is a versatile, non-destructive analytical technique which can be used for a variety of applications including: oxidation and reduction processes, biradicals and triplet state molecules, reaction kinetics, as well as numerous additional applications in several research fields, like chemistry or medicine. However, this technique can only be applied to samples having one or more unpaired electrons.

Spectroscopy is the measurement and interpretation of the energy difference between atomic or molecular states. According to Plank's law, electromagnetic radiation will be absorbed if:

$$\Delta E = hv \qquad (1)$$

where ΔE is the difference energetic difference between the two states, h is Planck's constant and v is the frequency of the radiation [13]. The absorption of this energy causes a transition of an electron from the lower energy state to the higher energy state [14]. In EPR spectroscopy the radiation used is in the gigahertz range. Unlike most traditional spectroscopy techniques, in EPR spectroscopy the frequency of the radiation is held constant while the magnetic field is varied in order to obtain an absorption spectrum [15].

The basis of EPR spectroscopy lies in the spin of an electron and its associated magnetic moment. When an electron is placed within an applied magnetic field, B, the two possible spin states of the electron have different energies. The lower energy state occurs when the magnetic moment of the electron, μ, is aligned with the magnetic field and the higher energy state occurs where μ is aligned against the magnetic field. The two states are labelled by the projection of the electron spin, M_S, on the direction of the magnetic field, where M_S = - ½ is the parallel, and M_S= + ½ is the antiparallel state (see Figure 6) [13].

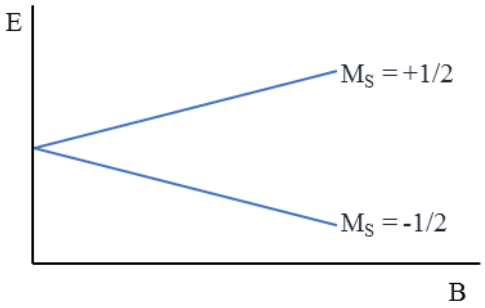

Figure 6. Energetic levels for a system with electron spin number ½.

So for a molecule with one unpaired electron in a magnetic field, the energy states of the electron can be defined as:

$$E = g\mu_B B M_S = \pm\frac{1}{2} g\mu_B B \qquad (2)$$

where g is the proportionality factor (or g-factor), μ_B is the Bohr magneton, B is the magnetic field and M_S is the electron spin quantum number. From this relationship, there are two important factors to note: the two spin state have the same energy when there is no applied magnetic field and the energy difference between the two spin states increases linearly with increasing magnetic field strength [15].

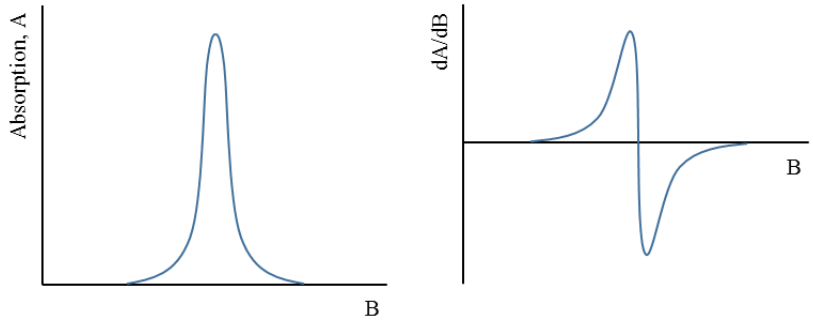

Figure 7. Theoretical absorption curve and its first derivative, in EPR spectroscopy.

As mentioned earlier, an EPR spectrum is obtained by holding the frequency of radiation constant and varying the magnetic field. Absorption occurs when the magnetic field tunes the two spin states so that their energy difference is equal to the incident radiation (see equation 1). This is known as the field for resonance. Figure 7 (left) shows the spectrum normally obtained in most spectroscopic techniques, as well as the typical EPR spectrum (right) presented as the first derivative of the absorption with respect to the applied

magnetic field. From this curve, three characteristic parameters of the radical species in the sample can be obtained, allowing their identification and quantification:

1. *G-factor*: also known as proportionality factor, this parameter gives information about the nature of the atomic or molecular orbital containing the unpaired electron [16]. Every radical presents a characteristic g-factor value, that can be calculated as:

$$g = \frac{h\nu}{\mu_B B} \tag{3}$$

2. *Hyperfine structure*: in addition to the applied magnetic field, unpaired electrons are also sensitive to their local environments. The hyperfine structure results from the magnetic coupling between the spin of the unpaired electrons and those magnetic nuclei ($M_S \neq 0$) near them, since these produce a local magnetic field at the electron. This kind of interaction leads to *2NI + 1* additional levels of energy for every different nuclei (different spin value) magnetically coupled to the electron, where *N* is the number of equivalent nuclei and *I* is the corresponding spin value [16], [17]. According to this explanation, the resulting spectrum of an EPR experiment would present *2NI+1* lines like the one showed in Figure 7 (right), depending on the chemical structure of the radical species in study. Moreover, lines in the spectrum could present different intensities and field separations between them, called hyperfine coupling constants. All of this would depend on the relative position of the corresponding magnetic nuclei in the radical molecule [16].

   Definitely, the hyperfine structure provides very important information about the number and identity of nuclei in a radical complex, as well as their distance from the unpaired electron. Because of that, all this data is very useful to identify the radical species present in the sample.

3. Amplitude or area: like in most spectroscopic techniques, the signal amplitude or area gives quantitative information about the sample. These parameters depends,

among others, on the concentration of the sample and the irradiation conditions [13].

Spin trapping procedures for singlet oxygen detection by EPR

As mentioned, the goal of the EPR analysis is to prove the singlet oxygen generation during the OPFR natural photodegradation process. This procedure, as explained earlier, is a suitable analytical technique to this purpose. But due to the short life of these reactive oxygen species, a direct EPR experiment is not possible in this case. Instead of that, indirect EPR analysis of $^1O_2$ by means of spin-trapping procedures should be performed.

In a spin-trapping assay, unstable free radical in solution reacts with a diamagnetic molecule, the spin trap, to form a relatively stable free radical called spin adduct. Once that occurs, the original free radical can be detected and identified by observing the EPR spectrum of the spin adduct, just as in a normal EPR experiment, since their characteristics (g-value, hyperfine structure, amplitude…) have been previously studied and are perfectly known [17]. Figure 8 shows a scheme of this experiment, applied to the case of study.

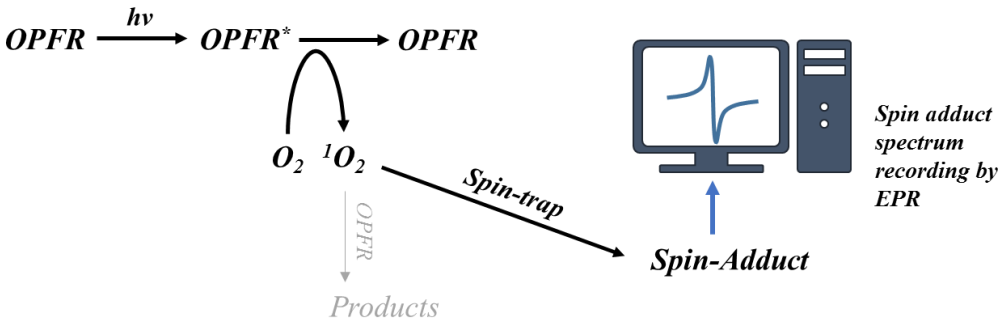

Figure 8. Scheme of a typical spin-trapping experiment for $^1O_2$ detection.

As observed, the process is very similar to the one described for photobleaching experiments. In both cases, an auxiliary compound (chemical probe or spin trap) is used to trap the radical and finally detected by means of a proper analytical technique.

2 Objectives

The aim of this project is to elucidate the natural photodegradation mechanisms of OPFR in superficial waters. Concretely, photosensitizer properties of some aryl phosphates and the role of singlet oxygen on sunlight degradation of this compounds are expected to be confirmed. Thus, the main objective was focused on the application of different procedures to demonstrate the photosensitizing properties of OPFR and the participation of singlet oxygen on the reaction mechanism. In order to do that, some specific objectives were stablished:

1. To study the viability to demonstrate the presence of singlet oxygen $^1O_2$, by means of chemical probe photobleaching experiments. This include:

    a. Selection of the probe.
    b. To adapt the operational conditions reported in bibliography to the project reaction system.

2. To perform spin-trapping procedures by using Electron Paramagnetic Resonance (EPR) in order to identify singlet oxygen in the reaction medium.

3 Materials and methods

3.1 Chemicals

The standards of 2-ethylhexyl diphenyl phosphate (EHDP) and trimethyl phenyl phosphate (TMPP) were purchased from Sigma Aldrich (Germany). Their chemical structures are presented in figures A.1-A.2 of Annex. 9,10-anthracenediyl-bis(methylene)dimalonic acid (ABMDMA), 2,2,6,6-tetramethyl-4-piperidone (4-oxo-TEMP) and furfuryl alcohol (FFA) were also purchased from Sigma Aldrich (Germany). Methanol and sodium hydroxide were acquired from Panreac (Spain).

In order to prepare the ABMDMA stock solution, 10 mg of this compound were dissolved in 200 mL of Milli-Q water. To dissolve ABMDMA completely, its corresponding sodium salt was prepared by adding the stoichiometric quantity of sodium hydroxide to the solution. In relation to OPFR stock solutions, 10 mg of each compound were dissolved separately in 100 mL of methanol to give final concentrations of 100 mgL^{-1}. The rest of reagents did not present insolubility problems in water, so the corresponding stock solutions were prepared at final concentrations of: 10 mM for FFA and 100 mM for 4-oxo-TEMP. All the solutions were stored in amber glass bottles and kept refrigerated.

3.2 Experimental setup

3.2.1 Photobleaching experiments

All photobleaching experiments were performed using simulated sunlight in a SolarBox® (Co.fo.me.gra 220 V, 50 Hz) system equipped with a Xe-OP lamp (Phillips 1 kW) and glass filters that cut off radiation with wavelengths under different values, as required.

For photobleaching experiments with ABMDMA an open, jacketed reactor (100 mL) and its corresponding magnetic stirrer were placed in the geometrical centre of the system, thus maximizing the direct irradiance over the reaction media. In order to maintain the temperature at 25 ºC, cold water from a reservoir tank was continuously pumped (peristaltic pump Ecoline VC-280®) into the reactor cooling jacked, and then recirculated back there. A complete scheme of the experimental setup is shown in Figure 9.

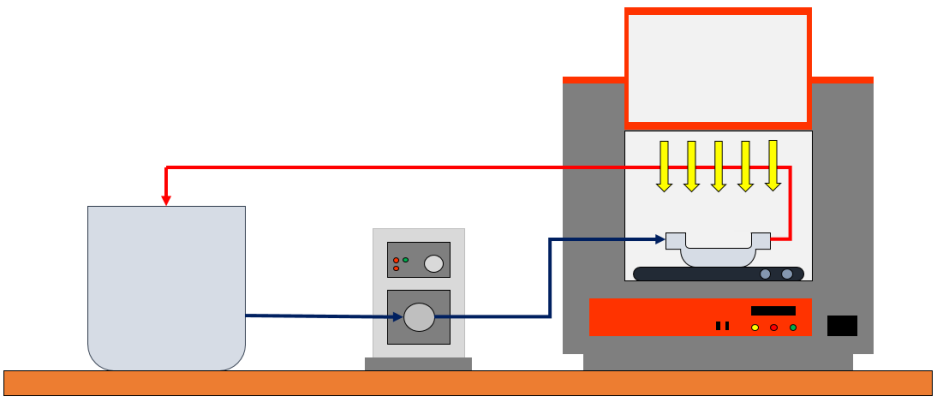

Figure 9. Experimental setup for photobleaching experiments.

For their part, photobleaching experiments with FFA were performed in a tubular reactor (2.11 cm x 24 cm) fed by means of a stirred and refrigerated reservoir tank, from where the reaction medium was continuously pumped and recirculated back there. Since this experimental setup is equal to the one employed in [10], details can be found there.

Reaction monitoring was carried out by UV-vis spectrophotometry (Hach DR 6000) or high performance liquid chromatography (Agilent Infinity 1260), depending on the chemical probe employed during the experiment. For HPLC analysis of FFA, a Mediterranean Sea18, 5 µm 25 cm x 0.46 cm (Teknokroma) column was used and the detection wavelenght was 220 nm. The mobile fase was 30% acetonitrile/70% phosphoric acid (pH 3).

3.2.2 Spin trapping experiments

All spin-trapping experiments (reaction and subsequent spectra recording by EPR) were carried out in a quartz tubular cell (reactor) placed on a Bruker EMX EPR spectrophotometer equipped with a super high-Q cavity (Bruker BioSpin GmbH, Rheinstetten, Germany). Spectra were recorded using an IBM-compatible computer interfaced with the spectrophotometer with the following instrument settings and conditions: 20 mW microwave power, 100 kHz modulation frequency, 1 G modulation amplitude, 20.48 ms time constant, 60 s scan time, and multiple scans of 100 G. As indicated, samples were placed in a quartz tubular cell and irradiated directly inside the microwave cavity of the spectrometer using a 500 kW Xe arc lamp. Radiation from the lamp was passed through a glass filter to remove wavelengths below 280 nm and also through a water filter, in order to remove the infrared fraction of the spectrum and maintain the reaction medium temperature at a constant value of 25 ºC.

Figure 10 shows a complete scheme of the experimental setup, which also serves as a block diagram for the whole process that constitutes the experiment. As mentioned, the tubular cell is placed in the cavity, where is irradiated with simulated sunlight. At the same time, the EPR system monitors the evolution of the sample by a continuous recording of its corresponding spectra, at different reaction times (signal accumulation with time). In order to do that, a microwave source sends its radiation to the sample, which

is exposed to a magnetic field inside the cavity. Microwaves reflected back from the cavity are routed to the detector, coming out as a signal that represents the absorption of the sample.

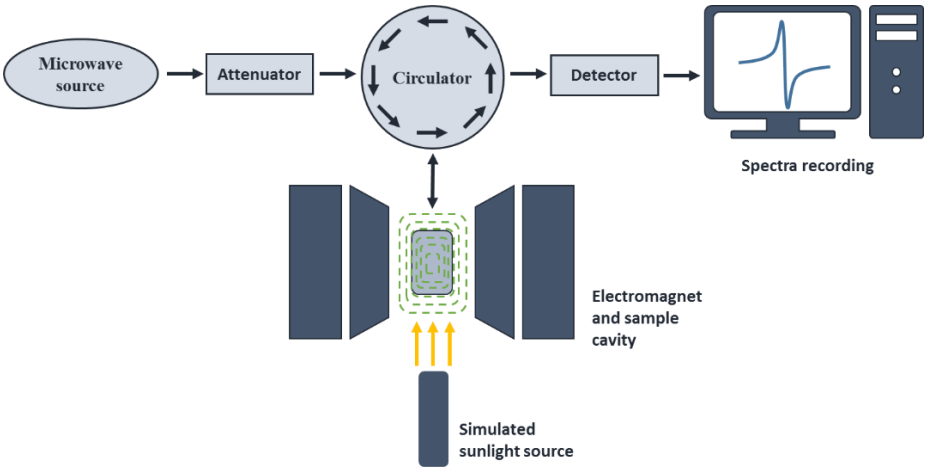

Figure 10. Experimental setup for spin trapping experiments by EPR spectroscopy.

4 Results and discussion

This section gathers all the experimental work carried out in order to demonstrate the implication of singlet oxygen in the natural photodegradation of OPFR. Since this was not a typical study with pre-stablished and well-working materials and methods, a considerable number of difficulties were taking place since the beginning of the project. Because of that, the following pages are organised respecting the real chronology of the study. That is, experiments, results, alternatives and possible solutions to any problem are presented and discussed just in the order in which they were thought and performed.

4.1 Absorption spectra of OPFR

EHDP and TMPP absorption spectra were obtained at 10 mgL^{-1} in a 10% methanol/water mixture. They are presented in Figure 11. As previously mentioned, both compounds have low absorption within the solar spectrum radiation, but it could be enough to initiate the photosensitization process. In fact, these chemicals are the ones that present higher

absorption levels among all the OPFR whose degradation was studied in [10], probably due to the aromatic rings on their chemical structures (see Figure A.1 and Figure A.2 of the *Supplementary material*). Thus one of them or both had to be responsible for initiate the indirect photodegradation mechanism earlier described and this is why they were selected for the experiments.

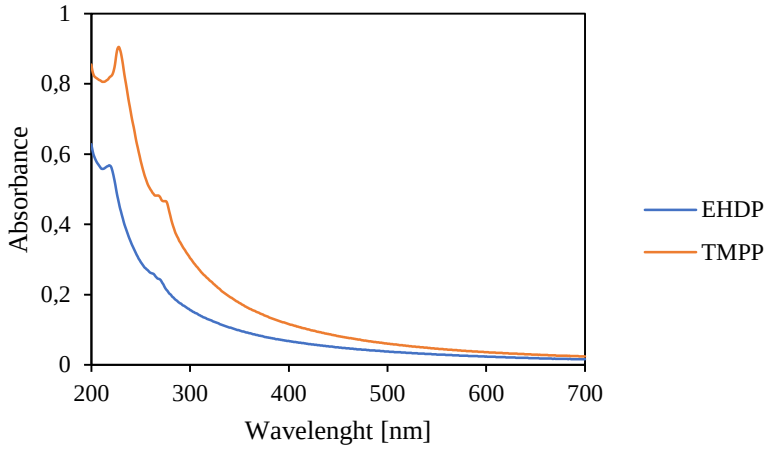

Figure 11. Absorption spectra of EHDP and TMPP.

4.2 Photobleaching experiments with ABMDMA

The first attempt to detect singlet oxygen in the reaction medium was carried out by means of photobleaching experiments. According to the previous literature, this procedure seemed to be simple, or at least simpler than spin-trapping experiments. So the first research efforts were focused on this method, and the first step was the chemical probe selection.

4.2.1 Selection of ABMDMA as the singlet oxygen detection probe

Several studies on different research fields have reported the use of 9,10-anthracenediyl-bis(methylene)dimalonic acid (ABMDMA) as chemical probe to monitor reactions involving singlet oxygen [18], [19], [20], [21]. ABMDMA is a water soluble derivative of anthracene that acts as a quencher for $^1O_2$, as Figure 12 illustrates.

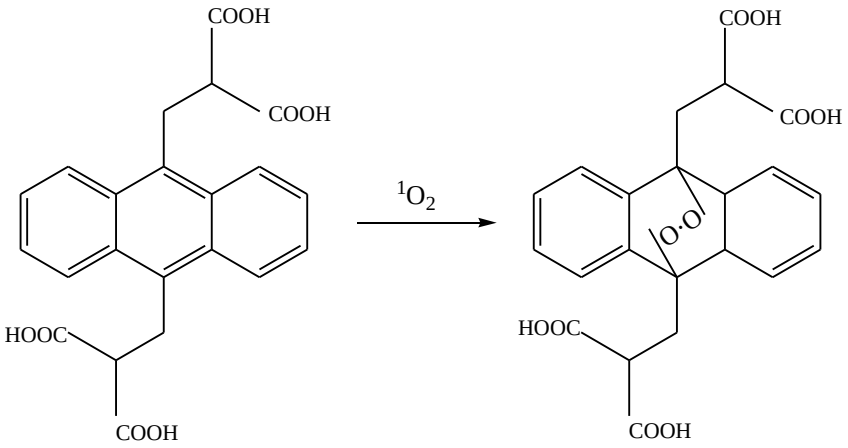

Figure 12. Singlet oxygen quenching by ABMDMA.

As previously described, ABMDMA photobleaching experiments to identify the presence of $^1O_2$ molecules would consist on irradiate a solution containing the chemical probe and a photosensitizer compound (aryl OPFR in the current case), and then observe the evolution of ABMDMA concentration along the reaction. Since the chemical probe presents a characteristic absorption peak at 400 nm (see Figure 13) and its corresponding endoperoxide not, a drop in the absorbance at 400 nm would indicate the generation of singlet oxygen and its subsequent quenching by ABMDMA. Because of the apparent simplicity of the experiment, choosing this probe seemed to be the best option.

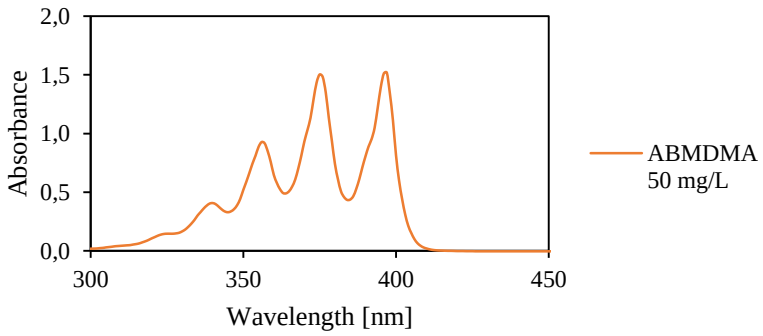

Figure 13. Absorption spectrum of ABMDMA in water.

As reported in literature [18], other chemical probes like 2-furoic acid and 9,10-anthracenedipropionic acid (ADPA) could be used with the same purpose and needed similar (and equally simple) analytical techniques for the reaction monitoring. Since ADPA is no longer manufactured and the furan derivative reaction with $^1O_2$ is notably slowly [18], ABMDMA was finally selected as detection probe for singlet oxygen.

Despite photobleaching experiments seem to present good chances of success, the operational conditions of the experimentation in the literature for ABMDMA photobleaching tests were quite different from the ones applied in OPFR photosensitizing conditions. Thus, in order to adequately perform the tests and obtain reliable results, the experiments had to be adapted to the required settings. The most important restrictions and inherent difficulties found prior starting the essays are detailed below, as well as some preliminary essays performed in order to find the most suitable experimental conditions.

Reactor scale

Due to the high price of ABMDMA (and EHDP), it was necessary to carry out all the experiments at small scale. That implied, principally, the use of a small volume of reaction (between 20 and 50 mL) and a low volume cuvette (160 µL) to carry out the corresponding spectrophotometric analysis. This volumetric restrictions had the next negative consequences on the experiments:

1. The reactor is open and presents a high surface of the reaction medium exposed to irradiation. Since the ratio area/volume of the reactor is relatively high, even with refrigeration some significant evaporative losses were expected at long experimental reaction times. If it is not possible to get results at short reaction time, a possible measure to reduce the error associated to this drawback would be to apply a correction factor to the chemical probe concentration, based on the remaining volume evolution experimentally obtained from an extra assay.

2. The cuvette volume is so small that essays were subjected to higher experimental error than with larger volume cuvettes. The presence of any foreign particle present in the solution, for instance coming from air, could provide wrong results.

Chemical probe stability with radiation

If ABMDMA quenching by $^1O_2$ is wanted to be observed, chemical probe should not be degraded by the effect of radiation, or at least light stability should be enough to

distinguish one effect from the other. From previous works it was known that ABMDMA is stable under irradiation of wavelength above 550 nm [19], but no studies were found in which this experiments were carried out with more energetic light. In the current case, radiation between 300-500 nm should be used in order to promote the photosensitization mechanism of aryl OPFR, since this is the range in which these compounds present a certain absorption level within the solar spectrum radiation [10]. Therefore, some stability test for ABMDMA were carried out.

ABMDMA and OPFR concentration

Since ABMDMA presents absorption in the range between 300-500 nm (as Figure 13 shows), a competition for light would probably be stablished between flame retardants and ABMDMA. If the main goal of the experiments was to observe the OPFR photosensitization process, an adequate molar ratio between the two compounds should be found in order to compensate the lower absorption levels presented by flame retardants in relation to ABMDMA. Therefore, OPFR should probably had equal or larger concentrations than the chemical probe at the beginning of the reaction. Preliminary experiments also focused on find a proper value of this parameter. In relation to the adequate molar ratio mentioned above, two additional restrictions had to be considered:

1. First, ABMDMA concentration should be large enough to be reliably measured by UV-Vis spectrophotometry. Thus, a minimum value had to be respected.

2. OPFR are not water soluble, so it would probably exist a maximum concentration value that cannot be exceeded if precipitation wanted to be avoided, even if the stock solutions of these compounds were made with methanol.

4.2.2 Determination of proper experimental conditions

As commented in last section, some test were carried out in order to find proper experimental conditions for ABMDMA photobleaching assays. Next, the most important results are shown and discussed.

Effect of radiation

Figure 14 exhibit the results of two ABMDMA stability experiments carried out with different filters which cut-off radiation below 280 and 400 nm, respectively. The employed concentration of the chemical probe was 50 mgL^{-1}, in water.

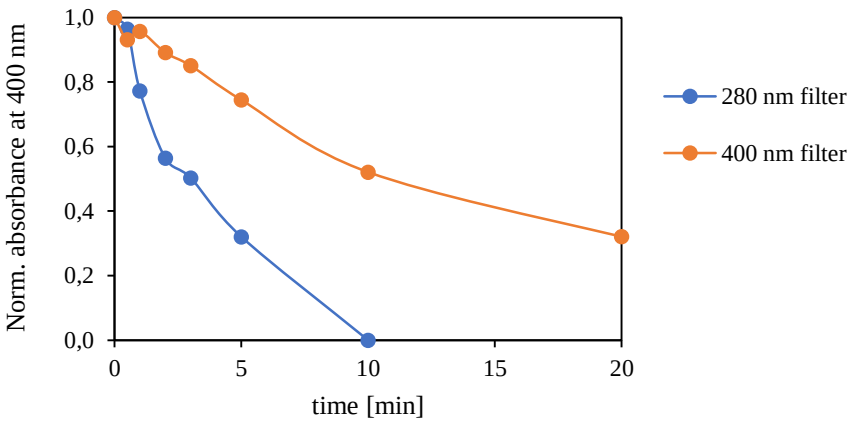

Figure 14. ABMDMA photo-stability under different irradiation conditions.

As expected, ABMDMA presented significant degrees of photodegradation in the two studied cases, being more stable when irradiated with longer wavelength light. As mentioned in previous sections, it would be ideal that this compound would remain totally stable so that OPFR photosensitizing effect could be more clearly observed, but this not seemed possible, according to the results obtained. Nevertheless, if $^1O_2$ is generated by photosensitization processes, as expected, its contribution to ABMDMA quenching would be more noticeable than direct photolysis, due to the higher kinetics typically shown by this radical species [11]. Observing that difference would be enough to demonstrate the initial hypothesis of this work, as previously stated in the literature [20].

Initial ABMDMA concentration

By means of several spectrophotometric tests, it was found that ABMDMA minimum concentration that could be reliably detected with this technique was 5 mgL^{-1}, so this value was fixed as the initial concentration of chemical probe. For lower concentrations, absorbance values were too low to work with and the experimental error was enhanced, causing the appearance of measurement instabilities.

4.2.3 Singlet oxygen detection by ABMDMA photobleaching

In order to determine a proper initial concentration of OPFR, some assays were carried out varying the molar ratio between the two compounds. Several values of this parameter were tested, being the most promising the ones with larger concentrations of OPFR, as expected. Figure 15 shows the degradation results obtained for ABMDMA: OPFR (a 50% mixture of EHDP and TMPP) molar ratios of 50:1, 5:1 and 1:1. All this experiments were performed employing the 400 nm filter, an initial ABMDMA concentration of 5 mgL^{-1} and the reaction time was increased to 20 minutes since the concentration of ABMDMA was lower and also its degradation rate.

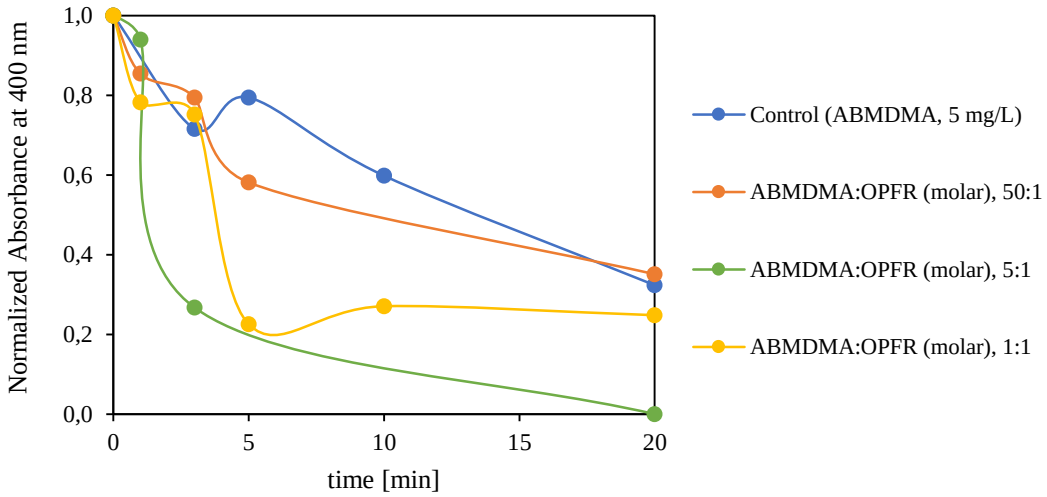

Figure 15. ABMDMA photobleaching in the presence of OPFR.

Process at a molar ratio of 50:1 exhibited a similar tendency than control experiment, so this means that this ABMDMA:OPFR ratio was not enough to observe the effect of flame retardant photosensitization on the chemical probe depletion process. On the other hand, degradation curves at molar ratios 5:1 and 1:1 showed an enhancement of the degradation rates at the beginning of the reaction, in comparison with the control experiment. As mentioned before, this had to be due to the photosensitizing effect of OPFR, which promoted singlet oxygen generation and therefore, the chemical quenching of ABMDMA. However, results are not reliable enough: for a molar ratio of 1:1, the process seemed to be slower in comparison with the reaction progress at a molar ratio of 5:1. In addition, the reaction seemed to stop after 10 minutes, according to the observed absorbance values from that moment. This estrange results could be consequence of the

low water solubility of flame retardants, which could introduce a further experimental difficulty added to those already set out previously.

Evaporative losses in all the experiments were about 10% of the initial volume. Since the recommended maximum volume loss in this kind of experiments is about 10% and the collected samples represented a total volume loss of approximately 5%, the evaporative losses were significant but not severe. Therefore, they were discarded as a possible cause for any abnormal result.

Finally, in order to get over the low solubility of OPFR in water, experiments were performed using methanol as ABMDMA and OPFR solvent. Although ABMDMA absorption spectrum of the probe did not change significantly in the new organic media, the absorption capacity of both OPFR diminished significantly (see Figure B.1 of the *Supplementary material*). This phenomenon, together with the higher volatility of methanol under high-power Xe-lamp discard the possibility of performing the experiments in alcoholic solutions.

4.3 Photobleaching experiments with FFA

After the initial imprecisions on photobleaching experiments with ABMDMA, it was clear that the reaction system in study presented too many restrictions and inherent difficulties that had to be overcome in order to obtain reliable results. With this purpose, two measures could be taken:

1. In order to remove the photo-instability of the chemical probe, it would be necessary to find another compound with a similar function, this time with no absorption over 280 nm.

2. To get over the OPFR insolubility problems, the methanol/water proportion in the reaction media could be increased. The higher the amount of methanol in the mixture, the higher the quantity of OPFR that can be contained in the solution.

4.3.1 Selection of FFA as the singlet oxygen detection probe

By means of some bibliographic research, it was found that furfuryl alcohol (FFA) has been widely used as a singlet oxygen detection probe in reaction systems containing chemicals with photosensitizing properties [22], [23], [24]. FFA is a furan derivative (see Figure A.3 of the *Supplementary material*) that, according to [25] has the following qualities:

1. It does not present direct photolysis or photosensitization. In order to check that, the UV-Vis spectrum of this compound was obtained (Figure 16).

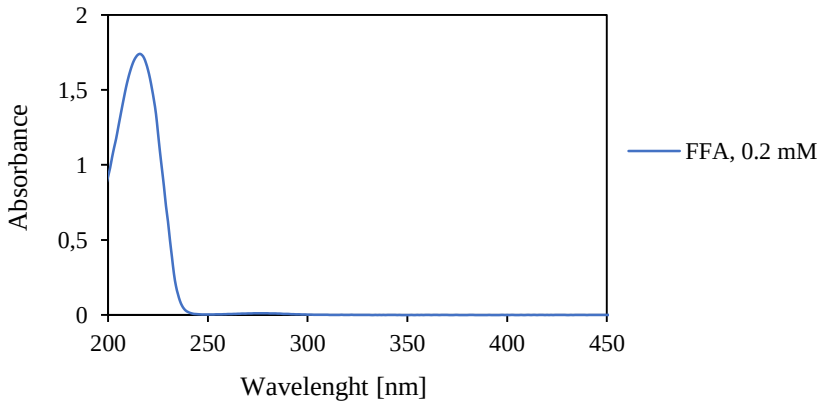

Figure 16. Absorption spectrum of FFA in water.

2. It presents high rate constant for reaction with $^1O_2$. Unlike what happens with ABMDMA, FFA does not react specifically with singlet oxygen, but its reaction kinetics with this ROS is (a priori) higher enough. Moreover, it has been demonstrated that this chemical does not quenches photosensitized molecules, so there should not be interference problems with excited OPFR.

3. It is highly water-soluble.

In view of the above, FFA seemed to accomplish the required qualities for a good chemical probe in the current case of study, and therefore it was presented as a good solution to the lack of photo-stability observed in the first round of photobleaching experiments. In addition, FFA presented a reasonable price that allowed to work with larger reaction volumes, thus minimizing the experimental error attributed to this factor.

In relation to the use of ABMDMA, only a disadvantage was observed: the monitoring of FFA concentration must be carried out by means of liquid chromatography. Due to the characteristics of the HPLC UV detector, the limit of quantification for FFA was between 0.05 and 0.1 mM. This value was about 5-10 times greater than the minimum ABMDMA concentration reliable measurable by UV-Vis spectroscopy. Details of the HPLC method, adapted from [22] and [23], have already been described and the corresponding calibration curve can be checked on Figure B.2 (*Supplementary material*).

4.3.2 Increase of the methanol/water ratio in the reaction medium

As mentioned, methanol proportion in the reaction medium was wanted to be increased in order to reduce OPFR insolubility problems and have a large amount of photosensitizer available. But as described on the last part of the experiments with ABMDMA (Figure B.1 of the *Supplementary material*), when the solution was entirely made with methanol, EHDP and TMPP lost completely their absorption over 280 nm.

Regardless of finding an explanation for this surprising phenomenon, some test were necessary to determine the absorption of both OPFR in relation to the methanol content in the solution. Thus, several UV-Vis spectra were obtained (concentration 0.25 mM), being the most representative ones presented in Figure 17 and Figure 18.

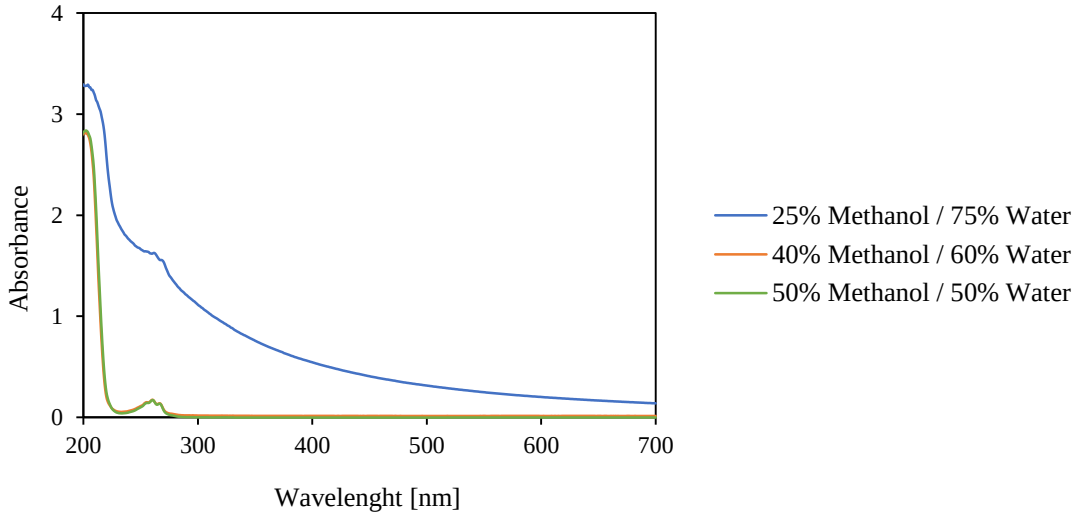

Figure 17. EHDP absorption spectrum with different solvent compositions.

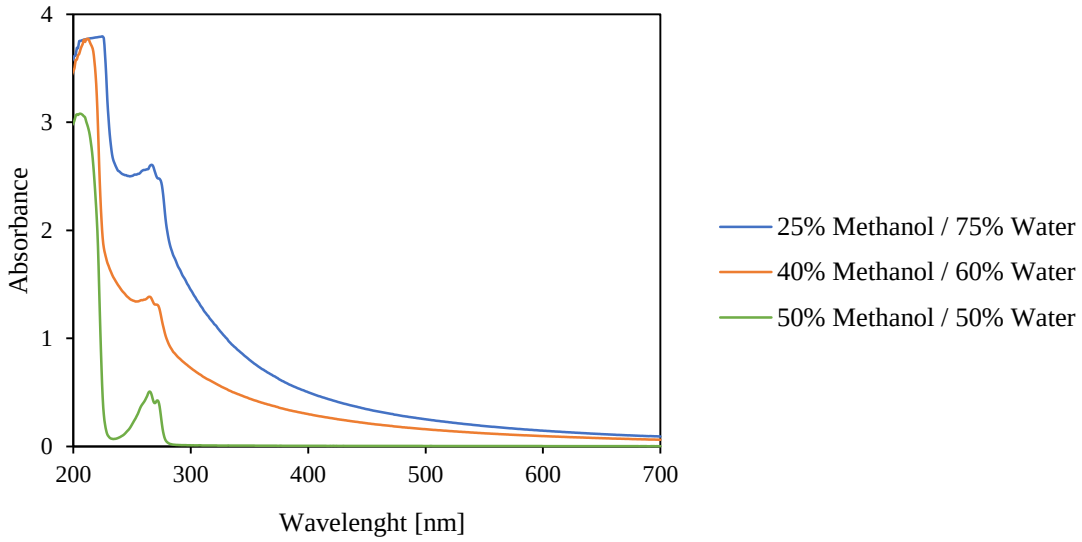

Figure 18. TMPP absorption spectrum with different solvent compositions.

As it can be observed, both chemicals lost gradually their absorption levels with an increasing content of methanol in the solvent mixture. This behaviour continues until the ratio is approximately 40% methanol / 60% water, for EHDP, and 50% methanol /50% water, for TMPP. From this value, absorption levels of OPFR drops dramatically. Being conservative and considering that the largest possible level of absorption is still needed to initiate the photosensitization process, it was decided to increase the content of methanol from 10 to 25% for the next experiments. It is important to remark that the difference between the absorption levels in both cases (with 10 or 25% of methanol) was insignificant.

4.3.3 Singlet oxygen detection with FFA photobleaching

Being the two main problems (probe photo-stability and OPFR insolubility) theoretically solved or reduced, the final step was to carry out several experiments with the intention of observing a decrease in FFA concentration, results that as explained, would demonstrate the hypothesis of the project.

OPFR concentrations were fixed to 0.25 mM, since this was the maximum concentration tolerated by the solution without observing precipitation. For its part, FFA initial concentration was fixed to 0.1 mM.

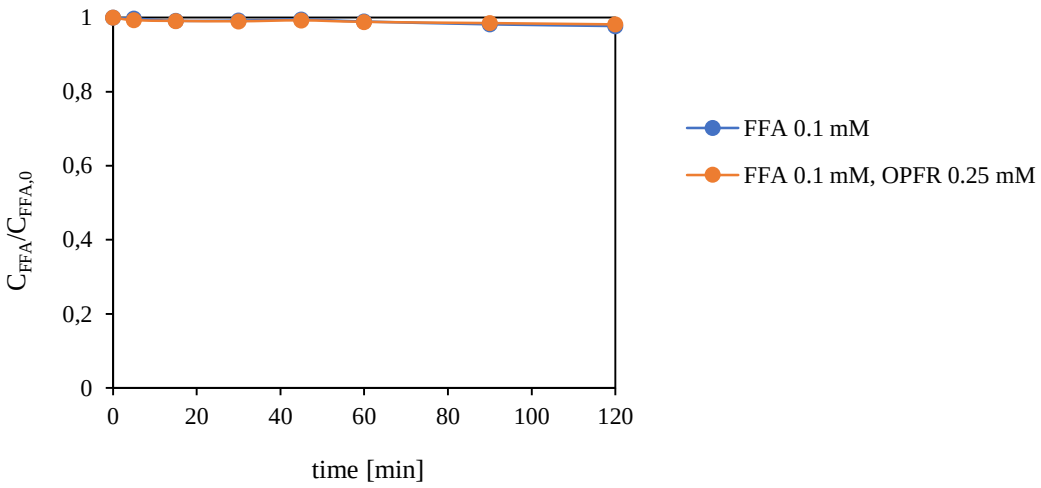

Figure 19. FFA photobleaching in the presence of OPFR.

As Figure 19 illustrates, differences between the control and the experiment with OPFR could not be observed. Several additional assays were performed, this time varying the molar ratio of concentrations between the two compounds. This measure had really no sense because FFA concentration does not competes for light (as happens with ABMDMA) and OPFR was already fixed to the maximum possible value. So as expected, same negative results were obtained and it was decided not to represent them.

Failure in FFA experiments could not be discussed by the same reasons that explained why ABMDMA photobleaching did not succeed. As stated before, the selection of a new chemical probe and the attempt of increasing the photosensitizer concentration to the maximum possible value should had overcome, or at least reduce, the main difficulties inherent to the reaction system in study. Because of that, during the last photobleaching experiments this set of complications should not have been presented. A possible explanation to the lack of success on these experiments would be related to the kinetics of the process. If singlet oxygen has to react with the chemical probe, a minimum concentration of this ROS should be constantly present in the reaction medium.

According to [26], the steady state concentration of this species would be equal to its formation rate divided by the sum of physical quenching and reactions with other species, as described by equation 4.

$$[\,^1O_2]_{SS} = \frac{k_a \Phi_{SO}[S]}{k_x[X] + k_d} \quad (4)$$

where k_a is the specific light absorbance of the reaction medium, S represents a photosensitizing molecule with a singlet oxygen quantum yield of Φ_{SO}, k_x represents the reaction rate between singlet oxygen and any species X present at the reaction medium (including the photosensitizer), while k_d is the rate of decay of oxygen back to its ground state due to quenching by water.

Adapting equation 4 to the current reaction system, S would represent OPFR and X would include FFA, but also OPFR and indirectly methanol. Thus, a competence for the reaction with singlet oxygen would be stablished between all these species. According to the results from [10], OPFR would present fast reaction kinetics with $^1O_2$, so it would be probable that this species react with most of the singlet oxygen being generated, thus minimizing its chemical quenching by FFA. For its part, the quenching of $^1O_2$ by water would present high kinetic constant ($2.5 \cdot 10^5$ s^{-1} [26]).

All of the above constitutes a too great disadvantage to have proper $^1O_2$ concentrations in the reaction medium, thus making quite difficult to observe the desired reaction between singlet oxygen and FFA. Moreover, the impossibility of observing an evolution of FFA concentration could be related to its initial quantity in the bulk solution, probably too large to observe small changes caused by $^1O_2$ quenching (in this case), but necessary for HPLC detection, as previously stated.

4.4 Spin-trapping experiments

After the lack of success with photobleaching, spin-trapping experiments were launched as the last attempt to prove the presence of singlet oxygen in the reaction system in study. Since this is a highly sensitive technique, even with very low concentrations of radicals in the bulk solution, it seemed to be a suitable procedure for the current case of study.

4.4.1 Selection of the spin-trapping agent

Unlike with photobleaching experiments, there was no doubt when a spin-trapping agent had to be chosen for singlet oxygen detection by EPR spectroscopy. Several works have reported the use of 2,2,6,6-tetramethyl-4-piperidone (4-oxo-TEMP) to this purpose [27], [28], [29], [30], [31], since singlet oxygen can oxidise this compound to the stable 2,2,6,6-tetramethyl-4-piperidone-1-oxyl (4-oxo-TEMPO), which is a spin adduct that and can be detected by EPR spectroscopy . Figure 20 illustrates the mentioned reaction.

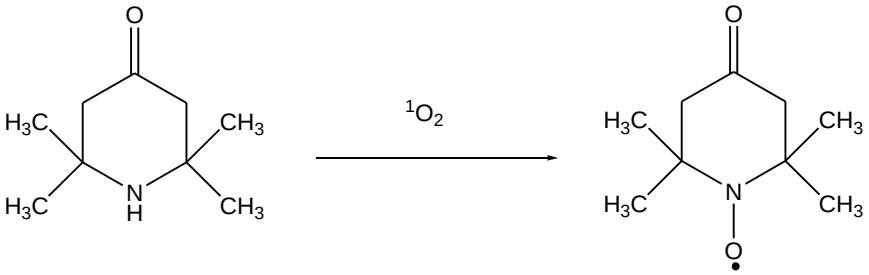

Figure 20. Generation of the spin adduct 4-oxo-TEMPO.

According to the EPR fundamentals previously described, 4-oxo-TEMPO spectrum would present an aspect like the one that Figure 21 exhibits.

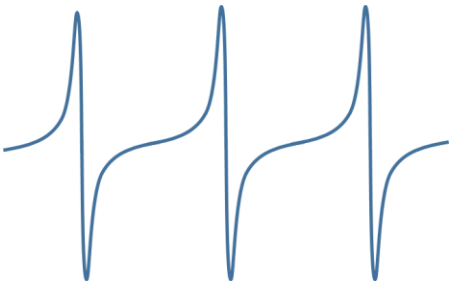

Figure 21. Theoretical EPR spectrum of 4-oxo-TEMPO.

In this case, the unpaired electron of the free radical species would only be sensitive to the magnetic spin of the ^{14}N nuclei (spin number 1), which is the nearest one [16]. Oxygen would not present magnetic coupling, since ^{16}O spin number is equal to 0. If as described, the appearing number of lines of an EPR spectra follows the rule *2NI+1*, the calculus in this case would be *2·1·1+1=3*. Thus, the predicted EPR spectrum would present, as shown, three equivalent EPR signals.

In addition to the spectrum shape, according to [32] and [33] the predicted g-value and hyperfine coupling constant for the corresponding signals would be 2.0054 and 16 G, respectively.

4.4.2 Singlet oxygen detection by spin-traping procedures

To finally perform the spin-trapping experiment, a solution of 4-oxo-TEMPO (25 mM) and the OPFR (0,25 mM, 1:1 EHDP and TMPP) was prepared in a methanol/water mixture. Water was previously bubbled with oxygen in order to assure an optimmumm concentration of this species in the reaction medium. A control experiment with only the spin-trapping agent was also performed, at the same conditions than the final experiment. (the only difference was the absence of OPFR). For all the experiments the irradiation time of the sample was 40 min. Results are shown in Figure 22.

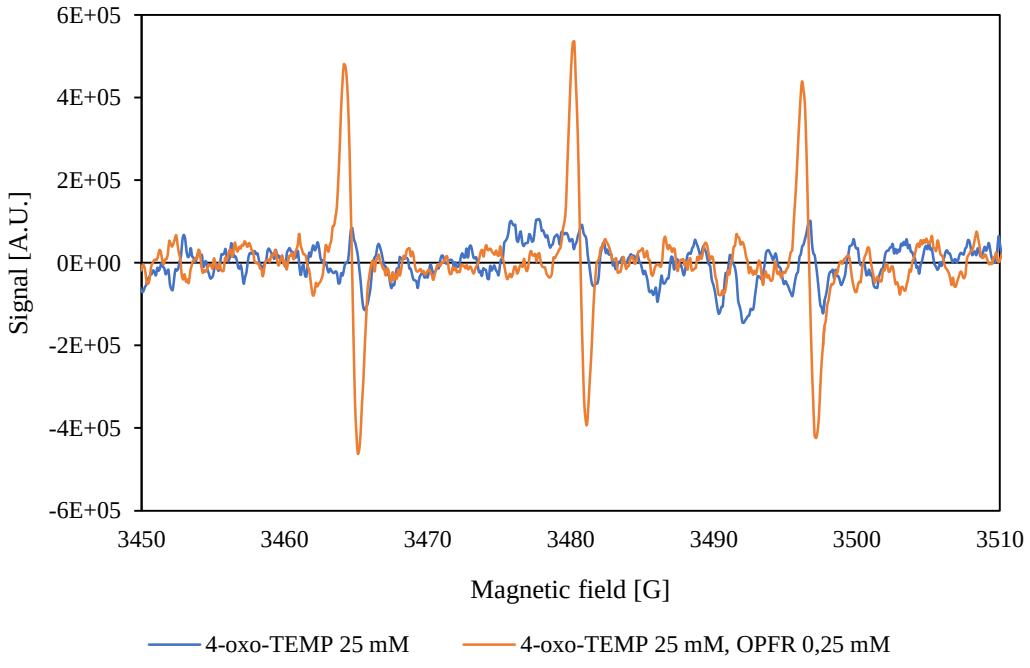

Figure 22. Experimental EPR spectrum of spin adduct 4-o-TEMPO.

As expected, the spectrum of the experiment with photosensitizers presented the shape above predicted, and a clearly difference in relation to the control experiment in terms of signal amplitude and area. This indicates the detection and identification of 4-oxo-TEMPO, and subsequently the generation and presence of singlet oxygen. With the aim

of assure the unequivocal identification of this species, the g-factor (equation 3) and the experimental hyperfine coupling constant were also calculated. The obtained results were 2.0056 and 16 G, respectively, two values practically equals to the expected ones.

The above results can also be presented as a time evolution of the accumulated signal, by using the results obtained by the EPR spectrophotometer at different reaction times. This can be observed in Figure 23. The graphic shows an almost lineal increase of the accumulated signal with time, which demonstrates that singlet oxygen production is sustained along the reaction.

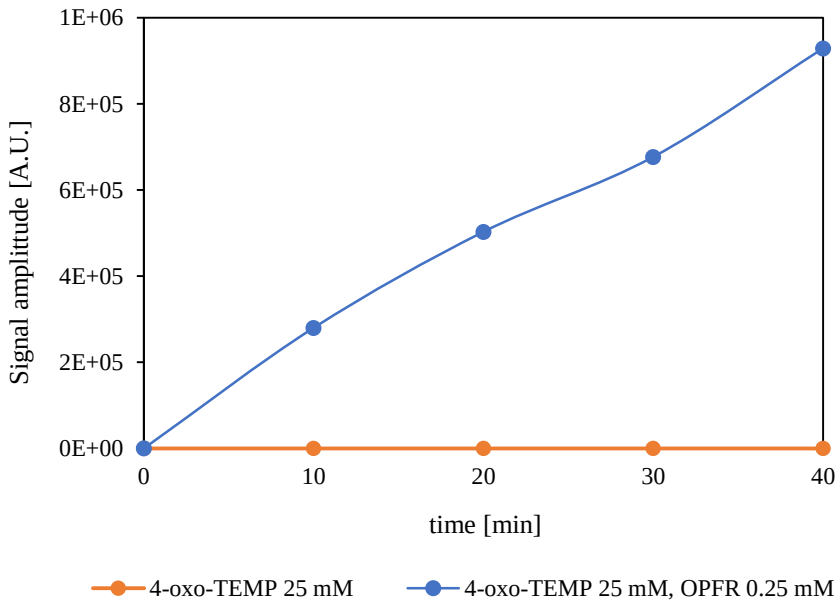

Figure 23. Accumulated EPR signal with time (4-o-TEMPO generation).

Success in these experiments and failure in the photobleaching ones could be consequence of the relative sensitivity of both methods and the kinetics of the reaction system towards the employed chemical probes or spin-trapping agent. During the photobleaching experiments discussion, it was concluded that singlet oxygen should be poorly present in the bulk solution, avoiding its detection by this assay. But this seems to be possible with the use of a very accurate and sensitive technique, which makes measurements continuously and at the same time in which the reaction and photosensitization process are taken place.

5 Conclusions

1. ABMDMA photobleaching experiments reported in literature needed to be adapted to the project requirements because their working conditions were not suitable with the project goals. This was not simple since some critical restrictions were present, like photo-instability of the chemical and OPFR insolubility.

2. Although several experiments were carried out in order to find proper experimental conditions for ABMDMA photobleaching experiments, the obtained results did not provide clear evidences of singlet oxygen generation. Therefore, it was concluded that photobleaching experiments with ABMDMA were not possible with this reaction system.

3. The absorption levels of OPFR are found to be dependent on the methanol content in the reaction medium. It was found that a 25% in volume is an adequate value, since this measure enhances the OPFR solubility in the reaction medium without a significant loss of the absorption capacity presented by these chemicals.

4. Although the two main problems of photobleaching were reduced, or even solved, experiments with FFA did not provide positive results. The key to this lack of success could be found on the kinetics of the reaction system: the poor presence of singlet oxygen caused by the fierce competition for this species presented by OPFR, FFA and the solvent, is a reasonable explanation to the failure on these experiments.

5. Based on the results obtained with photobleaching experiments, it is concluded that the reaction system in study is affected by too many factors that avoid to observe the desired reaction between oxygen singlet and the chemical probe, thus invalidating the employment of this kind of experiment for this purpose.

6. Spin-trapping procedures using 4-oxo-TEMPO detection as a method to identify the presence of singlet oxygen in the reaction medium have demonstrated to be

useful, since the obtained spectrum shows the shape and numerical parameters usually exhibited by this spin adduct.

7. Based on the evolution with time of EPR accumulated signal it can be concluded that singlet oxygen formation is sustained along the reaction. Thus, the photosensitization process starts once irradiation over the reaction medium is carried out and linearly increases with time.

8. The success exhibited by spin-trapping techniques seems to be explained by the great sensitivity of the EPR assays to the paramagnetic species, which allows to detect the presence of any of these structures in the reaction medium, even if their generation is limited by the inherent restrictions and difficulties showed by the reaction system in study.

6 Final recommendations

It is important to remark the fact that all the experiments performed during the project were carried out with mixtures of the two OPFR presumably responsible for the photosensitizing phenomenon. It was decided to do so because there were too many factors affecting the reaction system and this was the only way to assure that the photosensitizing process initiation would not be one of them.

Once demonstrated that aryl OPFR are involved in the natural photodegradation pathway of all OPFR, it would remain to perform the experiments separately for each one of this chemicals. This could provide information, for instance, about which of them are the main contributors to the singlet oxygen generation. Since the most satisfactory results has been achieved by spin-trapping procedures, in case of further interest it would be convenient to employ this technique to continue with the research.

References

[1] C. G. Daughton, "Non-regulated water contaminants: Emerging research," *Environ. Impact Assess. Rev.*, vol. 24, no. 7–8, pp. 711–732, 2004.

[2] A. Pal, K. Y. H. Gin, A. Y. C. Lin, and M. Reinhard, "Impacts of emerging organic contaminants on freshwater resources: Review of recent occurrences, sources, fate and effects," *Sci. Total Environ.*, vol. 408, no. 24, pp. 6062–6069, 2010.

[3] O. Segev, A. Kushmaro, and A. Brenner, "Environmental impact of flame retardants (persistence and biodegradability)," *Int. J. Environ. Res. Public Health*, vol. 6, no. 2, pp. 478–491, 2009.

[4] I. V der Veen and J. de Boer, "Phosphorus flame retardants: Properties, production, environmental occurrence, toxicity and analysis," *Chemosphere*, vol. 88, no. 10, pp. 1119–1153, 2012.

[5] G.-L. Wei, D.-Q. Li, M.-N. Zhuo, Y.-S. Liao, Z.-Y. Xie, T.-L. Guo, J.-J. Li, S.-Y. Zhang, and Z.-Q. Liang, "Organophosphorus flame retardants and plasticizers: sources, occurrence, toxicity and human exposure.," *Environ. Pollut.*, vol. 196, pp. 29–46, Jan. 2015.

[6] Clariant Produkte (Deutschland) GmbH, "The flame retardants market," 2014. [Online]. Available: http://www.flameretardants-online.com/web/en/106/7ae3d32234954e28e661e506e284da7f.htm. [Accessed: 12-May-2016].

[7] E. Koumaki, D. Mamais, C. Noutsopoulos, M. C. Nika, A. A. Bletsou, N. S. Thomaidis, A. Eftaxias, and G. Stratogianni, "Degradation of emerging contaminants from water under natural sunlight: The effect of season, pH, humic acids and nitrate and identification of photodegradation by-products," *Chemosphere*, vol. 138, pp. 675–681, 2015.

[8] J. Regnery "Occurrence and fate of organophosphorus flame retardants and plasticizers in urban and remote surface waters in Germany," *Water Res.*, vol. 44, no. 14, pp. 4097–4104, 2010.

[9] M. J. Watts and K. G. Linden, "Photooxidation and subsequent biodegradability of recalcitrant tri-alkyl phosphates TCEP and TBP in water," *Water Res.*, vol. 42, no. 20, pp. 4949–4954, 2008.

[10] J. Cristale, R. Dantas, A. De Luca, C. Sans, S. Esplugas, and S. Lacorte, "Role of oxygen and DOM in sunlight induced phototransformations of organophosphorous flame retardants in river water," *J. Hazard. Mater.*, 2016.

[11] M. C. DeRosa and R. J. Crutchley, "Photosensitized singlet oxygen and its applications," *Coord. Chem. Rev.*, vol. 233–234, pp. 351–371, 2002.

[12] E. Haggi, S. Bertolotti, and N. A. García, "Modelling the environmental degradation of water contaminants. Kinetics and mechanism of the riboflavin-sensitised-photooxidation of phenolic compounds," *Chemosphere*, vol. 55, no. 11, pp. 1501–1507, 2004.

[13] J. M. Hollas, *Basic atomic and molecular spectroscopy*. Cambridge : RSC, 2002.

[14] R. S. Drago, *Physical methods for chemists*. Ft. Worth [Pa.] [etc.] : Harcourt Brace Jovanovich College, 1992.

[15] J. A. Weil and J. R. Bolton, *Electron paramagnetic resonance : elementary theory and practical applications*. Hoboken (N.J.) : Wiley-Interscience, 2007.

[16] P. H. Rieger, *Electron spin resonance : analysis and interpretation*. Cambridge : RSC Publishing, 2007.

[17] A. Bencini and D. Gatteschi, *Electron paramagnetic resonance of exchange coupled systems*. Berlin [etc.] : Springer, 1990.

[18] V. Fabregat, M. I. Burguete, F. Galindo, and S. V. Luis, “Singlet oxygen generation by photoactive polymeric microparticles with enhanced aqueous compatibility,” *Environ. Sci. Pollut. Res.*, pp. 1–9, 2013.

[19] B. Zhao, J. J. Yin, P. J. Bilski, C. F. Chignell, J. E. Roberts, and Y. Y. He, “Enhanced photodynamic efficacy towards melanoma cells by encapsulation of Pc4 in silica nanoparticles,” *Toxicol. Appl. Pharmacol.*, vol. 241, no. 2, pp. 163–172, 2009.

[20] M. Wojtoniszak, D. Rogińska, B. Machaliński, M. Drozdzik, and E. Mijowska, “Graphene oxide functionalized with methylene blue and its performance in singlet oxygen generation,” *Mater. Res. Bull.*, vol. 48, no. 7, pp. 2636–2639, 2013.

[21] T. Tree-Udom, P. Thamyongkit and N. Wiratkasem “Harmonization of upconverting nanocrystals and photosensitizer for antimicrobial application,” *RSC Adv.*, vol. 5, no. 124, pp. 102416–102423, 2015.

[22] H. Fu, H. Liu, J. Mao, W. Chu, Q. Li, P. J. J. Alvarez, X. Qu, and D. Zhu, “Photochemistry of Dissolved Black Carbon Released from Biochar: Reactive Oxygen Species Generation and Phototransformation,” *Environ. Sci. Technol.*, vol. 50, no. 3, pp. 1218–1226, 2016.

[23] J. Brame, M. Long, Q. Li, and P. Alvarez, “Trading oxidation power for efficiency: Differential inhibition of photo-generated hydroxyl radicals versus singlet oxygen,” *Water Res.*, vol. 60, pp. 259–266, 2014.

[24] E. Erdim, A. R. Badireddy, and M. R. Wiesner, “Characterizing reactive oxygen generation and bacterial inactivation by a zerovalent iron-fullerene nano-composite device at neutral pH under UV-A illumination,” *J. Hazard. Mater.*, vol. 283, pp. 80–88, 2015.

[25] W. R. Haag, J. Hoign??, E. Gassman, and A. Braun, “Singlet oxygen in surface waters - Part I: Furfuryl alcohol as a trapping agent,” *Chemosphere*, vol. 13, no. 5–6, pp. 631–640, 1984.

[26] S. Mostafa and F. L. Rosario-Ortiz, “Singlet oxygen formation from wastewater organic matter,” *Environ. Sci. Technol.*, vol. 47, no. 15, pp. 8179–8186, 2013.

[27] A. Miyaji, M. Kohno, Y. Inoue, and T. Baba, “Singlet oxygen generation during the oxidation of L-tyrosine and L-dopa with mushroom tyrosinase,” 2016.

[28] H. Yuying, A. Jingyi, and J. Lijin, “Effect of structural modifications on photosensitizing activities of hypocrellin dyes: EPR and spectrophotometric studies,” *Free Radic. Biol. Med.*, vol. 26, no. 9–10, pp. 1146–1157, 1999.

[29] R. Konaka, E. Kasahara, W. C. Dunlap, Y. Yamamoto, K. C. Chien, and M. Inoue, “Irradiation of titanium dioxide generates both singlet oxygen and superoxide anion,” *Free Radic. Biol. Med.*, vol. 27, no. 3, pp. 294–300, 1999.

[30] V. Gómez-Vidales, G. Granados-Oliveros, A. Nieto-Camacho and M. Reyes-Solís “Cacalol and cacalol acetate as photoproducers of singlet oxygen and as free radical scavengers , evaluated by EPR spectroscopy and TBARS †,” *R. Soc. Chem.*, vol. 4, pp. 1371–1377, 2014.

[31] Y. Zhao, Q. Xia, J. J. Yin, H. Yu, and P. P. Fu, “Photoirradiation of polycyclic aromatic hydrocarbon diones by UVA light leading to lipid peroxidation,” *Chemosphere*, vol. 85, no. 1, pp. 83–91, 2011.

[32] J. MOAN and E. WOLD, “Detection of singlet oxygen production by ESR,” *Nature*, vol. 279, no. 5712, pp. 450–451, May 1979.

[33] Y. Lion, E. Gandin, and A. Vorst, “On the production of nitroxide radicals by singlet oxygen reaction: an EPR study,” *Photochem. Photobiol.*, vol. 31, no. 4, pp. 305–309, Apr. 1980.

Supplementary material

A. **Chemical structures**

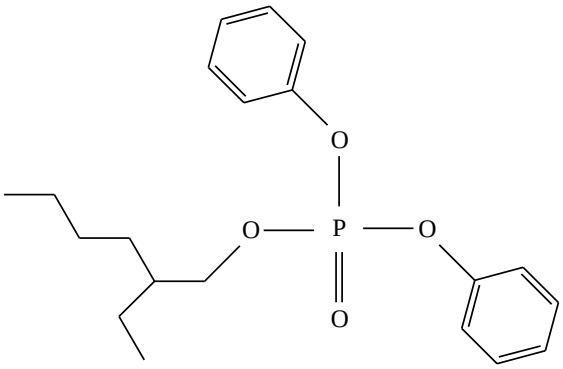

Figure A.1. Chemical structure of EHDP.

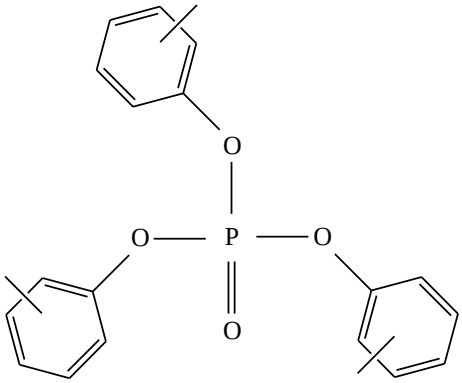

Figure A.2. Chemical structure of TMPP.

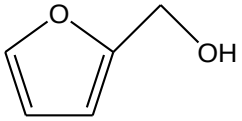

Figure A.3. Chemical structure of FFA.

B. **Experimental graphs**

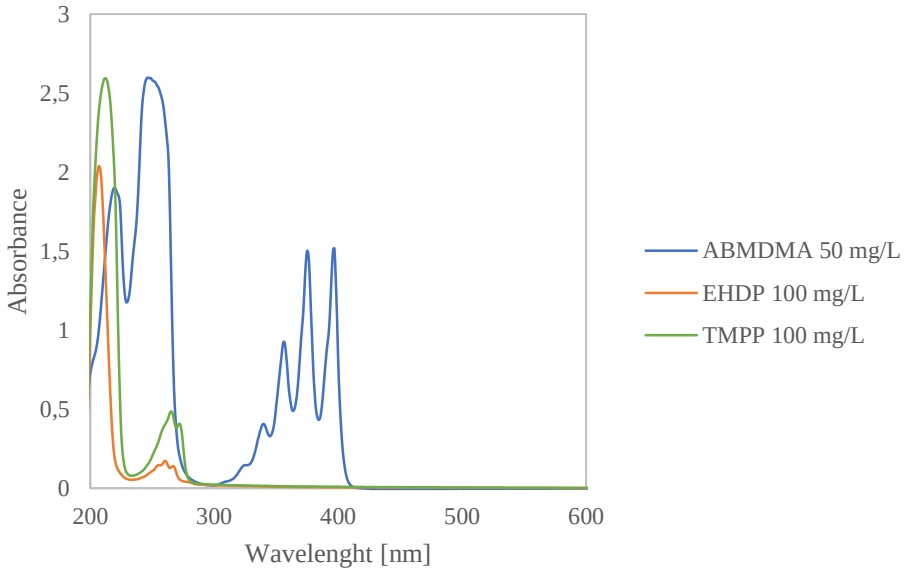

Figure B.1. ABMDMA and OPFR absorption spectra in methanol solution.

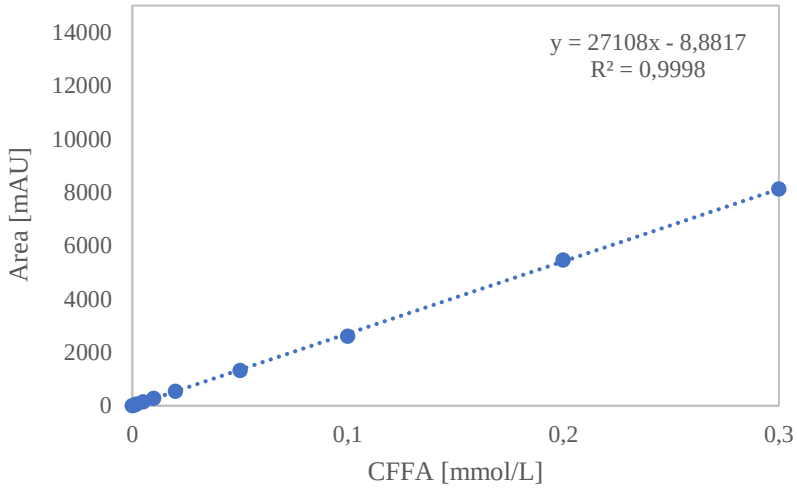

Figure B.2. HPLC calibration curve for FFA.